# Synthesis of PAM/$TiO_2$ Composite Microspheres with Hierarchical Surface Morphologies

Xiaojun Wang, Daodao Hu,* and Juxiang Yang

*Key Laboratory for Macromolecular Science of Shaanxi Province, School of Chemistry and Materials Science #94, Shaanxi Normal University, Xi'an City 710062, Shaanxi Province, P. R. China*

*Received October 26, 2006. Revised Manuscript Received March 12, 2007*

PAM/$TiO_2$ composite microspheres with hierarchical surface structures were synthesized by the reaction between tetrabutyl titanate (TBOT) located within porous polyacrylamide (PAM) microgels and water in a moist atmosphere. The morphology and composition of the composite microspheres were characterized by scanning electron microscopy (SEM), thermogravimetric analysis (TG), Fourier transform infrared spectroscopy (FI-IR), X-ray diffraction (XRD), $N_2$ absorption analysis, and mercury porosimetry, respectively. The results indicated that the composite microspheres, with different hierarchical surface morphologies, could be obtained by controlling the cross-linking degree of the porous PAM microgels, the relative humidity of the gas phase, the amount of residual impregnation liquid, and the TBOT concentration in the porous PAM microgels. Although the surface morphologies of the composite microspheres are varied, the morphologies are typically divided into three categories: (1) wrinkled surfaces covered with large dense $TiO_2$ particles; (2) porous structures sparsely suffused with large $TiO_2$ particles along the fringes and inner walls of the porous channels; and (3) macroporous surfaces with small $TiO_2$ particles distributed ubiquitously. The incorporation of $TiO_2$ particles into PAM microgels resulted in an obvious increase in specific surface area, and the pore size distribution of the microspheres depended strongly on the size of $TiO_2$ particles. The method described herein provides a potential way for fine-tuning the morphology and surface property of composite microspheres. Additionally, this method can be used to fabricate various composite materials through altering the precursor and/or polymeric microgel template.

## 1. Introduction

Porous materials are the kinds of materials that have uniform pore size and an ordered network in space.[1] Because of their unique advantages, such as high surface areas and a porous network, porous materials have potential applications in the areas of photoelectron material, heterogeneous catalysis, absorption, separation, biomedicine, microreactor, and so forth.[2−6] Hence, porous materials have become the subject of intensive research. Microporous molecular sieves, as high selectivity catalysts, are wildly used in the petroleum industry. However, there have been some restrictions in their application because some molecules are too large to enter into the small pores or some macromolecules forming in the network cannot easily get away from the pore to result in some side reactions. The novel family of molecular sieves called M41S was reported by the researchers at Mobil Research and Development Corporation in the 1990s; these mesoporous (alumino) silicate materials, with well-defined pore sizes of 15 ± 100 Å, break past the pore-size constraint (<15 Å) of microporous zeolites. The extremely high surface areas (>1000 $m^2\ g^{-1}$) and the precise tuning of pore sizes are among the many desirable properties that have made such materials the focus of great interest.[7] However, because of the simplex constituents of the molecular sieves and the finite adjustability in pore size, the mesoporous molecular sieves cannot be satisfied with the diversified functions expected in material applications. Therefore, the studies of porous materials with different textures and pore sizes have been attracting the interest of numerous researchers.

The template method is the main approach for the preparation of porous materials.[8−10] According to the template technique used, the template method is generally divided into two kinds, depending on which template technique is used. (1) The materials with pore channels are prepared by in situ aggregation, using surfactant as the template. The synthesis of mesoporous molecular sieves is a typical example. (2) The templates are embedded in a matrix, followed by post-treatment to selectively eliminate them via calcinations or solvent etching. For this method, the inorganic or polymeric materials could be used as matrix

* Corresponding author. E-mail: daodaohu@snnu.edu.cn.

(1) Holland, B. T.; Blanford, C. F.; Do, T.; Stein, A. *Chem. Mater.* **1999**, *11*, 795.
(2) Dabrowski, A. *Adv. Colloid Interface Sci.* **2001**, *93*, 135.
(3) Fornasieri, G.; Badaire, S.; Backov, R.; Olivier, M. M.; Zakri, C.; Poulin, P. *Adv. Mater.* **2004**, *16*, 1094.
(4) Cooper, A. I. *Adv. Mater.* **2003**, *15*, 1049.
(5) Martinez, C. J.; Hockey, B.; Montgomery, C. B.; Semancik, S. *Langmuir* **2005**, *21*, 7937.
(6) Laberty-Robert, C.; Long, J. W.; Lucas, E. M.; Pettigrew, K. A.; Stroud, R. M.; Doescher, M. S.; Rolison, D. R. *Chem. Mater.* **2006**, *18*, 50.
(7) Back, J. S.; Vartuli, J. C.; Roth, W. J.; Leonowicz, M. E.; Kresge, C. T; Schmitt, K. D.; Chu, C. T-W.; Olson, D. H.; Sheppard, E. W.; McCullen, S. B.; Higgins, J. B.; Schlenker, J. L. *J. Am. Chem. Soc.* **1992**, *114*, 10834.
(8) Kresge, C. T.; Leonowicz, M. E.; Roth, W. J. *Nature* **1992**, *359*, 710.
(9) Archibald, D. D.; Mann, S. *Nature* **1993**, *364*, 430.
(10) Xia, Y. N.; Gates, B.; Yin, Y. D.; Lu, Y. *Adv. Mater.* **2000**, *12*, 693.

10.1021/cm062561g CCC: $37.00 
Published on Web 04/24/2007

or templates. According to the shape of the porous matrix, the porous materials are divided into membrane,[11−14] rod,[15−16] block,[17−19] and sphere shapes.[20−24] For example, Wang prepared the porous membrane materials by solvent etching.[11] The materials were synthesized using silica sphere colloid crystals as the template. The air between the spheres was replaced by poly(amic acid), and the templates were removed by the application of hydrofluoric acid. Kazuhiro Sasahara fabricated macroporous ceramic thick films consisting of nanosized particles by a modified sol−gel method, using polymethylmethacrylate (PMMA) microspheres as a template.[17] PMMA microspheres were first deposited on an oxidized silicon substrate. Precursor solutions permeated into the openings of the template layer in vacuo and were then air-dried at room temperature. The composite layers were then subjected to heat treatment in air in order to remove the core PMMA templates by thermal decomposition and then to oxidize the precursor frameworks. In this method, a macroporous structure could be controlled by varying the particle size of PMMA microspheres and the concentration of precursor solutions. He Xiue-dong et al. reported a novel and efficient approach to synthesiing cagelike polymer microsphere materials with hollow core/porous shell structures by self-assembly of sulfonated PS latex particles at the monomer droplet interface.[20] The swelling of the PS latex particles by the oil phase provides a driving force to develop a hollow core. The latex particles also serve as a porogen that will disengage automatically during polymerization, leaving behind a uniform porous shell. The size of the microspheres and the pore size of the shell can be easily adjusted. The obtained microspheres may find potential applications in the fabrication of functionalized composites for controlled release systems and catalytic applications.

As well as the above-mentioned template methods, for preparation of porous materials, other methods have been reported. For example, porous $SnO_2$ nanostructures are prepared by thermal decomposition of the solution composed of dibutyltin dilaurate and acetic acid. The $SnO_2$ nanoplates have a wormlike structure due to the aggregation of small primary nanoparticles. These nanoplates finally assemble into larger particles, and hierarchically porous structured materials are obtained.[24] The formation of pores should be attributed to the space occupied by acetic acid and the gas given off during the decomposition process. It should be noted that such porous nanostructures are obtained without the use of any template and structure-directing reagents such as surfactants. Techniques based on the use of highly compressed gases or supercritical fluid have been developed to form polymeric materials such as microspheres, porous fibers, and porous foams.[14] Hideto Matsuyama et al. reported the method for preparation of the microporous polystyrene membrane by phase separation with supercritical $CO_2$. The supercritical $CO_2$ was used as the nonsolvent for polystyrene. The dry membrane was obtained without collapse of the structure after the pressure was diminished. Hiwatari and co-workers reported a method for the preparation of macroporous polymeric films by pulling a substrate from the chloroform solution of copolymer (St/(PEG) to a moist atmosphere. Macroporous structures were attributed to the phase separation caused by condensed water droplets.[12] Di Li et al. demonstrated the feasibility of the spray pyrolysis technique for preparation of N−F-co-doped $TiO_2$ (NFT) powders with a porous and acidic surface.[22] The mechanism for the formation of the porous particle morphology of the NFT powders was ascribed to the enormous gas evolution from $NH_4F$ during $TiO_2$ particle formation and the template role played by the $NH_4Cl$. Wang and co-workers developed an approach to fabricate porous crystalline $TiO_2$, $SrTiO_3$, and $BaTiO_3$ spheres.[23] The formation of porous structures of these crystalline $TiO_2$, $SrTiO_3$, and $BaTiO_3$ spheres could be explained by a mechanism analogous to the Kirkendall effect. All research mentioned above indicates that the porous materials could be papered by some other method besides the template method.

Although there are lots of studies on the preparation of the porous materials, there are few reports about the polymer/inorganic composite microspheric materials that have porous structures. The polymeric hydrogel has three-dimensional network structures.[25] Additionally, polymeric hydrogel materials are widely used in drug-release control, microreactor, chemical sensors, enzyme fixation, biochip, etc.[26−30] Hence, the preparation of the polymer/inorganic composite microspheric materials with porous structures would provide a new approach for exploring new functional materials. On the basis of these considerations, we would expect to prepare the porous composite microspheric materials through deposition of inorganic components on the polymeric microgel with porous structure.

More recently, our group proposed a polymeric microgel template method for preparation of composite microspheric materials. Employing poly(*N*-isopropylacrylamide-*co*-acrylic acid) (P(NIPAM-*co*-AA), poly(*N*-isopropylacrylamide-*co*-methacrylic acid) (P(NIPAM-*co*-MAA), polyacrylamid (PAM)

(11) Wang, J.; Lin, B. P.; Yuan, C. W. *Acta Chim. Sin.* **2004**, *62*, 1019.
(12) Hiwatari, K. I.; Serizawa, T.; Seto, T. *Polym. J* **2001**, *33*, 669.
(13) Nabeta, M.; Sano, M. *Langmuir* **2005**, *21*, 1706.
(14) Matsuyama, H.; Yano, H.; Maki, T.; Teramoto, M.; Mishima, K.; Matsuyama, K. *J. Membr. Sci.* **2001**, *194*, 157.
(15) Nishihara, H.; Mukai, S. R.; Yamashita, D.; Tamon, H. *Chem. Mater.* **2005**, *17*, 683.
(16) Lee, S.; Jeon, C.; Park, Y. *Chem. Mater.* **2004**, *16*, 4292.
(17) Sasahara, K.; Hyodo, T.; Shimizu, Y.; Egashira, M. *J. Eur. Ceram. Soc.* **2004**, *24*, 1961.
(18) Collins, A.; Carriazo, D.; Davis, S. A.; Mann, S. *Chem. Commun.* **2004**, 568.
(19) Breulmann, M.; Davis, S. A.; Mann, S.; Hentze, H. P.; Antonietti, M. *Adv. Mater.* **2000**, *12*, 7.
(20) He, X. D.; Ge, X. W.; Liu, H. R.; Wang, M. Zh.; Zhang, Zh. Ch. *Chem. Mater.* **2005**, *17*, 5891.
(21) Zhang, Z. P.; Shao, X. Q.; Yu, H. D.; Wang, Y. B.; Han, M. Y. *Chem. Mater.* **2005**, *17*, 332.
(22) Li, D.; Haneda, H.; Hishita, S.; Ohashi, N. *Chem. Mater.***2005**, *17*, 2588.
(23) Wang, Y. W.; Xu, H.; Wang, X. B.; Zhang, X.; Jia, H. M.; Zhang, L. Z.; Qiu, J. R. *J. Phys. Chem. B* **2006**, *110*, 13835.
(24) Zhao, Q. R.; Zhang, Z. G.; Dong, T.; Xie, Y. *J. Phys. Chem. B* **2006**, *110*, 15152.
(25) Saunders, B. R.; Vincent, B. *Adv. Colloid Interface Sci.* **1999**, *80*, 1.
(26) Siegel, R. A.; Firestone, B. A. *Macromolecules* **1988**, *21*, 3254.
(27) Ilnaubm, F.; Tanaka, T.; Kokufuta, E. *Nature* **1991**, *349*, 400.
(28) Kajiwara, K.; Ross-Murphy, S. B. *Nature* **1992**, *355*, 208.
(29) Weissman, J. M.; Sunkara, H. B.; Tse, A. S.; Asher, S. A. *Science* **1996**, *274*, 959.
(30) Holtz, J. H.; Holtz, J. S. W.; Munro, C. H.; Asher, S. A. *Anal. Chem.* **1998**, *70*, 780.

**Scheme 1. Procedure for Preparation of PAM/$TiO_2$ Composite Microspheres**

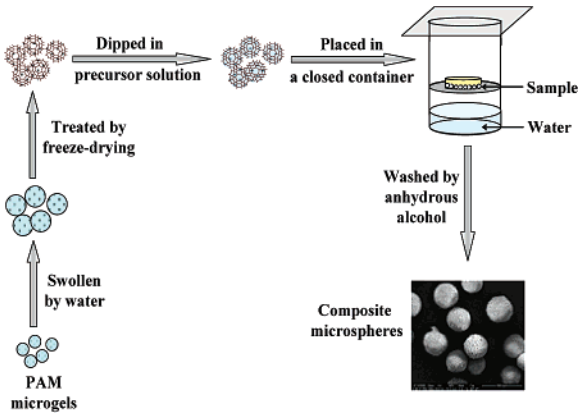


or poly(*N*-isopropylacrylamide) (PNIPAM) as templates, several interesting polymeric composite microspheres, with various patterned surface structures, have been successfully synthesized.[31−36] On the basis of these research results and applications of $TiO_2$ in photocatalysis, adsorptive separation, and environmental protection,[34−40] in this paper, we report a novel and efficient approach to synthesize composite microspheric material with hierarchical structures by in situ depositions of $TiO_2$ particles on the porous PAM microgels. The overall synthetic procedure is shown in Scheme 1.

The first step is to prepare the porous PAM microgels by the freeze-drying treatment of water-swelled PAM microgels. The porous microgels are then immersed in a mixture of anhydrous alcohol and tetrabutyl titanate (TBOT). After that, the immersed microgels are put in a moist atmosphere to make TBOT carry out hydrolysis and condensation. The results indicate that the composite microspheres, with different hierarchical surface morphologies, could be prepared by altering some parameters, including the concentration of the cross-linker (*N*,*N*′-methylene bisacryamide (BA)) in preparation of the PAM microgels, the amount of the residual impregnation liquid in the porous microgels, the precursor concentration in the impregnation liquid, and the humidity in the gas phase. Generally, the morphologies are typically divided into three categories: (1) wrinkled surfaces covered with large dense $TiO_2$ particles; (2) porous structure sparsely suffused with large $TiO_2$ particles along the fringes and inner walls of the porous channels; (3) macroporous surfaces with small $TiO_2$ particles distributed ubiquitously. On the basis of this protocol, the preparation of composite microspheres with different surface patterns, as well as the surface covered by $TiO_2$ particles in different sizes, could be achieved. Moreover, this technique would be suitable for the fabrication of various composite materials by altering the precursor and polymeric microgels template. The remarkable feature of this protocol is that composite microspheres can be prepared on the micrometer scale, which makes separation feasible. Additionally, the particles sizes on the surface of the composite microspheres approach the submicrometer scale, even at a nanometer scale. The pores sizes of the composite microspheres are therefore controllable within the range of micrometer to nanoscale.

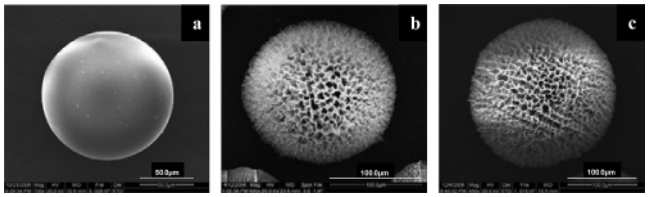


**Figure 1.** SEM images of (a) the water-swollen PAM microgels washed with alcohol, (b) the water-swollen PAM microgels after freeze-drying, and (c) the freeze-dried PAM microgels after being washed with alcohol.

## 2. Experimental Section

**2.1. Materials.** Acrylamide (AM) was purified by recrystallization in acetone. *N*, *N*′-methylene bisacryamide (BA), *N*,*N*,*N*′,*N*′-tetramethylenediamine (TMEDA), cyclohexane, acetone, tetrabutyl titanate (TBOT), ammonium persulfate (APS), and anhydrous alcohol were of analytical grade. All these chemicals were used without further purification. Water used in the experiments was double-distilled.

**2.2. Preparation of PAM Microgels.** PAM microgels were prepared according to the literature.[36] A typical synthesis is as follows: 70 mL of cyclohexane and 0.52 g of Span-80 were added to a 150 mL three-neck flask equipped with a mechanical stirrer and a nitrogen inlet. The mixture was stirred under nitrogen purging until the surfactant was uniformly dispersed. At the same time, 1.20 g of AM, 0.048 g of BA, and 1 mL of 18% APS dissolved into 5 mL of double-distilled water were added to the mixture. The mixture was then stirred continuously under a nitrogen atmosphere. The reaction was initiated by the addition of the promoter, which was 1 mL of the 5% TMEDA aqueous solution, and the mixture was stirred (380 rpm) at 20 °C for 4 h. The PAM microgels were collected and washed alternatively with double-distilled water and alcohol, and the white product was dried overnight under ambient conditions. The SEM images of the resulting PAM microgels are shown in Figure 1. The different cross-linking degree of PAM microgels could be obtained by altering the amount of cross-linker (BA). Some conditions for the preparation of PAM microgels with different cross-linking degrees are shown in Table 1.

**2.3. Preparation of PAM Porous Microspheres.** PAM microspheres with porous structures were prepared by the freeze-drying treatment. A typical preparation is as follows: 0.1 g of PAM microgel was swollen by adding 8 mL of double-distilled water and then the sample, after being quenched in liquid nitrogen, was freeze-dried by an ALPHA1-2 freeze-drying instrument at −55 °C for 12 h. The PAM microgels with porous structures were finally obtained. The porous PAM microgels with different pore sizes were gained when PAM microgels, prepared in different amounts of the cross-linker (BA), were treated by freeze-drying. The typical SEM images of the freeze-dried PAM microgels with different cross-linking degrees are shown in Figure 2.

(31) Bai, C. L.; Fang, Y.; Zhang, Y.; Chen, B. B. *Langmuir* **2004**, *20*, 263.
(32) Fang, Y.; Bai, C. L.; Zhang, Y. *Chem. Commun.* **2004**, *7*, 804.
(33) Zhang, Y.; Fang, Y.; Wang, S. *J. Colloid Interface Sci.* **2004**, *272*, 321.
(34) Zhang, Y.; Fang, Y.; Lin, S. Y.; Liu, J.; Yang, J. L. *Acta Phys.−Chim. Sin.* **2004**, *20*, 1.
(35) Bai, C. L.; Wang, S.; Zhang, Y.; Fang, Y. *Shaanxi Normal Univ.* (*Nat. Sci. Ed.*) **2003**, *31*, 62.
(36) Yang, J. X.; Fang, Y.; Bai, C. L.; Hu, D. D. *Chin. Sci. Bull.* **2004**, *19*, 2026.
(37) Cheng, X. J.; Chen, M.; Wu, L. M.; Gu, G. X. *Langmuir* **2006**, *22*, 3858.
(38) Eiden-Assmann, S.; Widoniak, J.; Maret, G. *Chem. Mater.* **2004**, *16*, 6.
(39) Nakashima, T.; Kimizuka, N. *J. Am. Chem. Soc.* **2003**, *125*, 6386.
(40) Meyer, U.; Larsson, A.; Hentze, H. P.; Caruso, R. A. *Adv. Mater.* **2002**, *14*, 1768.

**Table 1. Some Conditions for the Preparation of PAM/TiO$_2$ Microspheres and PAM Microspheres[a]**

| PAM microgel sample | amount of BA (g)[b] | TBOT concentration in ratio of TBOT to alcohol (V/V)[c] | vacuuming time (min)[c] | ratio of water to anhydrous alcohol (V/V)[c] |
|---|---|---|---|---|
| Figure 1 | 0.072 | | | |
| Figure 2 | 0.036 (a),0.048 (c) 0.072 (e), 0.084 (g) | | | |
| Figure 3 | 0.048 | 0.02 (a), 0.01 (c) 0.005 (e), 0.003 (g) | 0 | 1:0 |
| Figure 4 | 0.048 | 0.003 | 10 (a), 20 (c) 30 (e), 40 (g) | 1:0 |
| Figure 5 | 0.048 | 0.003 | 0 | 1:0 (a), 7:3 (c) 1:1 (e), 3:7 (g) |
| Figure 6 | 0.084 (a), 0.072 (c) 0.048 (e), 0.036 (g) | 0.003 | 0 | 1:0 |

[a] All factors selected in the column head row of the table stem from the following considerations. (1) Different amounts of BA for the preparation of PAM microgels with different cross-linking degrees. (2) Different vacuuming times for altering the amount of residual impregnation solution. (3) Different volume ratios of alcohol to water for changing the humidity level of the gas phase. (4) Different TBOT concentrations for adjusting the rate of hydrolysis. [b] The other conditions for the preparation of PAM microgels are the same as those in section 2.2 in the text. [c] The other conditions for the preparation of PAM/TiO$_2$ composite microspheres are the same as those in section 2.4 in the text.

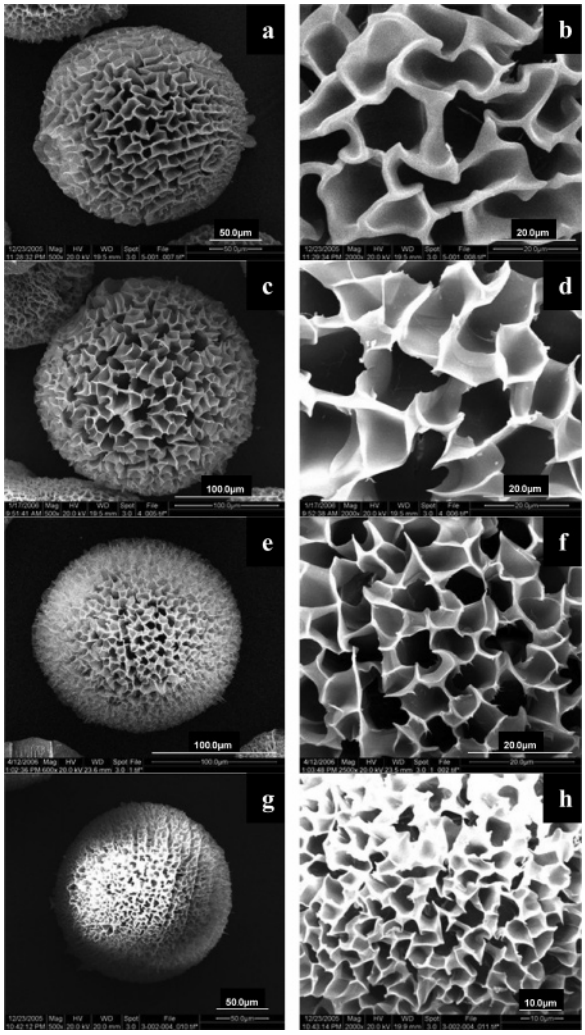


**Figure 2.** SEM images of the water-swollen PAM microgels with different cross-linking degrees after the freeze-drying. The cross-linking degrees are controlled by change in BA content: (a, b) 0.036, (c, d) 0.048, (e, f) 0.072, and (g, h) 0.084 g.

**2.4. Preparation of PAM/TiO$_2$ Composite Microspheres.** The composite microspheres of PAM/TiO$_2$ were commonly prepared by the following steps. At room temperature, 0.1 g of the freeze-dried PAM microgels was saturated with 10 mL of tetrabutyl titanate (TBOT) anhydrous alcohol solution (2.5%) in a laboratory dish, and this dish was then placed in a closed beaker containing water for 10 h. After being washed with anhydrous alcohol, the white PAM/TiO$_2$ composite microspheres were obtained. The preparation process is shown in Scheme 1. The PAM/TiO$_2$ composite microspheres with different hierarchical surface morphologies were prepared by altering some conditions (see Table 1). These conditions include the cross-linking degree of the PAM microgels, the humidity of the gas phase in the closed beaker, the amount of residual impregnation solution in the freeze-dried PAM microgels, and the TBOT concentration in the impregnation solution. In all the conditions mentioned above, the cross-linking degree and the TBOT concentration are easily controlled. The cross-linking degree could be changed by means of controlling the amount of BA in the preparation of PAM microgels. In the experiment, the amounts of BA selected were 0.5, 0.7, 1.0, and 1.2%. Comparatively, the humidity of the gas phase and amount of residual impregnation solution in the freeze-dried PAM microgels were difficult to be accurately controlled. To explore the effect of the two factors on surface morphologies of PAM/TiO$_2$ composite microspheres, we relatively adjusted the humidity and the amount of residual impregnation solution, employing the following methods. To control the humidity in the gas phase, we placed the mixture of anhydrous alcohol and water in different volume ratios in the closed beaker to create a different level of humidity in the gas phase. In the experiment, 0:1, 3:7, 1:1, and 7:3 anhydrous alcohol to water volume ratios were used. The method used for altering the amount of residual impregnation solution in the freeze-dried PAM microgels should be good not only in efficiently controlling the amount of residual solution but also in uniformly immersing the freeze-dried PAM microspheres.

The following process that we proposed meets the above-mentioned requirement. The freeze-dried PAM microgels are first saturated with TBOT anhydrous alcohol solution to make all of the microgels uniformly immersed, and the immersed microgels are then vacuumed for a given time so that the solvent is uniformly volatilized from all immersed microgels and the solvent in all microgels is efficiently controlled. In the experiment, the vacuuming times for adjusting the amount of residual impregnation liquid are 0, 10, 20, 30, and 40 min. The different conditions for the preparation of PAM/TiO$_2$ composite microspheres are shown in Table 1.

**2.5. Characterization.** The morphologies of the PAM microgels, the freeze-dried PAM microgels, and the PAM/TiO$_2$ composite microspheres were examined by Philips scanning electron microscopy (SEM) using an accelerating voltage of 20 kV (the samples were coated with a thin layer of gold before measurement). The elements in the samples were probed by the EDX analysis accessory to the scanning electron microscopy (SEM). The IR spectra were recorded on an AVTAR360 Nicolet Fourier transform infrared (FT-IR) spectrometer using a KBr pellet. Thermogravimetric analyses (TGA) were performed using a SDT Q600 V8.0 Build 95 instrument. The composite powders were heated to 750 °C in oxygen at a scan rate of 5 °C/min, and the observed mass loss was attributed to the quantitative pyrolysis of the polymeric component.

The X-ray diffraction (XRD) spectra were taken from $2\theta$ angles from 2 to 70° at a scan rate of 0.02°/min. The accelerating voltage and electric current were 35 kV and 40 mA, respectively. Considering that there are both macropores and micropores in the composite microspheres, $N_2$ adsorption and mercury porosimetry were used to measure some pore parameters of the composite microspheres. Nitrogen adsorption measurements were performed, using a ZXF-06 instrument, utilizing Barrett−Emmett−Teller (BET) calculations for the surface area. Porosity measurements were performed by mercury porosimetry using AutoPore IV 9500, version 1.07, over a pressure range of 0.10 to 30 000.00 psia.

## 3. Results and Discussion

**3.1. Morphology of PAM Microgels.** On the basis of the PAM microgels as templates to prepare the composite microspheres, it is necessary to explore the differences in the morphologies of the PAM microgels prepared or treated in different conditions, because the morphologies of the PAM composite microspheres strongly depend on that of the templates. The different conditions for the preparations of PAM microgels are shown in Table 1. The SEM images are shown in Figure 1, which include the water-swollen PAM microgels after being washed with alcohol and the water-swollen PAM microgels after being treated by freeze-drying.

It can be seen in Figure 1 that the water-swollen PAM microgels, after being washed with alcohol, are perfectly spherical with a diameter of less than 100 $\mu$m (see Figure 1a) and that their surfaces are smooth. The water-swollen PAM microgels, after being treated by freeze-drying, exhibit porous structures (see Figure 1b), and their porous structures did not change much after being washed by alcohol (see Figure 1c) and the diameter of the freeze-dried PAM microgels is about 200 $\mu$m. These results will be interpreted in the following section.

It is not difficult to understand that the swelling behavior of PAM microgels strongly depends on the cross-linking degree, and the cross-linking degree forcefully affects the porous structure of the freeze-dried PAM microgels. Therefore, the freeze-dried PAM microgels with different cross-linking degrees were prepared, so that some information on the morphologies of the freeze-dried PAM microgels as templates is expectedly obtained. Some conditions for preparation of the PAM microgels with different cross-linking degrees are shown in Table 1, and the SEM images of the resulting water-swollen PAM microgels after the freeze-drying treatment are shown in Figure 2. It clearly demonstrates that the porous microspheres exhibit a regular change in morphologies with an increase of cross-linker. The microspheres, after the freeze-drying treatment, are distinct porous structures, as we expected. Furthermore, with the increase in the cross-linker (amounts of BA in Figure 2 are (a) 0.036, (c) 0.048, (e) 0.072, and (g) 0.084 g), the diameter of the microspheres decreases (the diameters in Figure 2 are about (a, c) 200 $\mu$m, (d) 180 $\mu$m, and (g) 150 $\mu$m), the pore size gradually becomes smaller, and the pore wall becomes thinner (see Figure 2b, d, f, h).

R.P. Washington has reported on the hydrogels with porous structures after freeze-drying treatment by liquid nitrogen quencher.[41] Matsuo have provided the formation mechanism of the spongy porous structures using PNIPAM hydrogels as an example.[42] Hydrogels with porous structures, attributable to the nonergodic behavior of kinetic concentration fluctuations before forming hydrogels, phase separation, and instantaneous thermodynamic concentration fluctuations. PAM microgel is a sort of typical hydrogel and the formation mechanism of porous structures is similar to that of PNIPAM hydrogels. PAM microspheres have porous structures using BA as a cross-linker, and the polymeric structures formed by the pore wall are between the branched polymer chain and the polymer network in the space. The acrylamide groups on the polymeric chain have a favorable ability to form stronger hydrogen bonding with water and the pore wall has stronger absorption of water under the solvation of abundant acrylamide groups. At the same time, the capillarity of the pore has strengthened the ability to absorb water. When the water-swollen PAM microgels were treated by alcohol, the hydrogen bonds between the water molecules and the PAM polymeric chains were weakened so that water left the pore wall of the polymer network. Simultaneously, the hydrogen bonds among the acrylamide groups formed on the polymeric chain. The effects derived from treatment by alcohol resulted in the collapse of the porous structures. All of the microspheres were shrunk during the shrinkage of the pore wall, resulting in the microsphere surface becoming smooth, as shown in Figure 1a. There has been a report of an analogous phenomenon using PAA as a model.[43] The water in the polymeric network and in the pore wall composed of network polymeric chains was instantaneously solidified because of the liquid nitrogen quencher. It was then treated by freeze-drying, so that the solidified water left the microspheres by turning from a solid state into a gas state. Therefore, the microspheres with porous structures could be finally obtained, as shown in Figure 1b. On the basis of the above explanation, the observations (see Figure 1c) that the porous structure of the freeze-dried PAM microspheres did not change very much after being washed by alcohol can be understood because the effect of alcohol on the distortion of polymeric networks in the dried PAM microgels is negligible.

The increase in the cross-linking degrees of polymeric networks by increasing the amount of cross-linker in the polymeric reaction system leads to enhancing the rigidity of the pore walls of the polymeric microspheres. As a result, the pore walls become thinner and the pore sizes become smaller because of a decrease in the swelling degree of polymeric backbone network. On the basis of this explanation, the SEM images shown in Figure 2 are easily understood. It is shown from the above results, that the PAM microspheres with porous structures can be easily prepared by the freeze-drying process of the water-swollen PAM microgels, and that the pore size of the microspheres can be effectively adjusted by controlling the amount of cross-linker in the polymeric reaction system.

(41) Washington, R. P.; Steinbock, O. *J. Am. Chem. Soc.* **2001**, *123*, 7933.
(42) Matsuo, E. S.; Orkiszj, M.; Sun, S. T.; Li, Y.; Tanaka, T. *Macromolecules* **1994**, *27*, 6791.
(43) Tanaka, T.; Fillmore, D.; Sun, S. T.; Nishio, I.; Swislow, G.; Shah, A. *Phys. Rev. Lett.* **1980**, *45*, 1636.

**3.2. Morphology of PAM/$TiO_2$ Composite Microspheres.** According to the procedure we proposed for the preparation of PAM/$TiO_2$ composite microspheres in Scheme 1, the water-swollen PAM microgels treated by freeze-drying are first saturated with TBOT anhydrous alcohol solution and the immersed microgels are then placed in a moist atmosphere to cause TBOT in the microgels to hydrolyze. To control the morphology of the composite microspheres, some factors related to the preparation of the PAM/$TiO_2$ composite microspheres should be considered. Some factors shown in Table 1 were selected in our experiments, including the amount of residual impregnation liquid in the template microgels, humidity in gas phase, cross-linker degree of PAM microgels, and TBOT concentration in the impregnation liquid. The PAM/$TiO_2$ composite microspheres were prepared in the light of these conditions. As expected, the PAM/$TiO_2$ composite microspheres with a regular change in morphology were obtained. Generally, the composite microspheres exhibit regular spherical morphologies, and the surface morphology is of hierarchical structure. The average diameter of the composite microspheres is nearly equal to that of the templates. The results on the morphologies of the composite microspheres prepared under different conditions are discussed separately as follows.

**Influence of TBOT Concentration on the Morphology of PAM/$TiO_2$ Composite Microspheres.** Considering the fact that the alcohol had no effect on the porous structures of the template microgels, TBOT alcohol solution was selected for the immersing of the template microgels. Additionally, TBOT concentration might affect the morphology of the composite microspheres because incorporation of $TiO_2$ was carried out by hydrolysis of TBOT on the template microgels. So, the effect of TBOT concentration on the morphology of the composite microspheres should be investigated. Figure 3 shows the SEM images of PAM/$TiO_2$ composite microspheres prepared in different TBOT concentrations when the other experimental conditions were unchanged. All conditions are shown in Table 1. The TBOT concentrations in volume ratio of TBOT to alcohol are 0.02, 0.01, 0.005, and 0.003, respectively. It is clearly demonstrated in Figure 3 that the surface morphology of PAM/$TiO_2$ composite microspheres appears with regular variety, and that the diameter of the composite microspheres is about 150−180 $\mu$m. The surface of the composite microspheres is densely covered by $TiO_2$ particles, in case of high TBOT concentration. With the decrease of TBOT concentration, the number of $TiO_2$ particles deposited on the composite microspheres decreases, $TiO_2$ particles tendentiously deposit on the inner walls of the pores, and the surface morphology of the composite microspheres gradually appears as an obvious macroporous structure. Additionally, the $TiO_2$ particle size decreases with a decrease in TBOT concentration. In images a and g of Figure 3, the diametric ranges of $TiO_2$ particles are about 0.76−1.1 and 0.42−0.83 $\mu$m, respectively. These phenomena would be explained as follows. In the case of the higher value of the TBOT to alcohol volume ratio, the volatilizing rate of alcohol is relatively slower. As a result, there is enough residual impregnation liquid in the pore of the template microgels to facilitate mobility of the hydrolytes for the formation of $TiO_2$ particles and to increase in particle size. Contrarily, the volatilizing rate of alcohol in the case of the lower ratio is relatively faster in making less residual impregnation liquid in the template microgels, which leads to difficulties in the formation of $TiO_2$ particles and in the increase of particle size. Additionally, in this case, the residual impregnation liquid is mainly located in the pores, which makes $TiO_2$ particles dominantly form in the pores with less deposit at the surface.

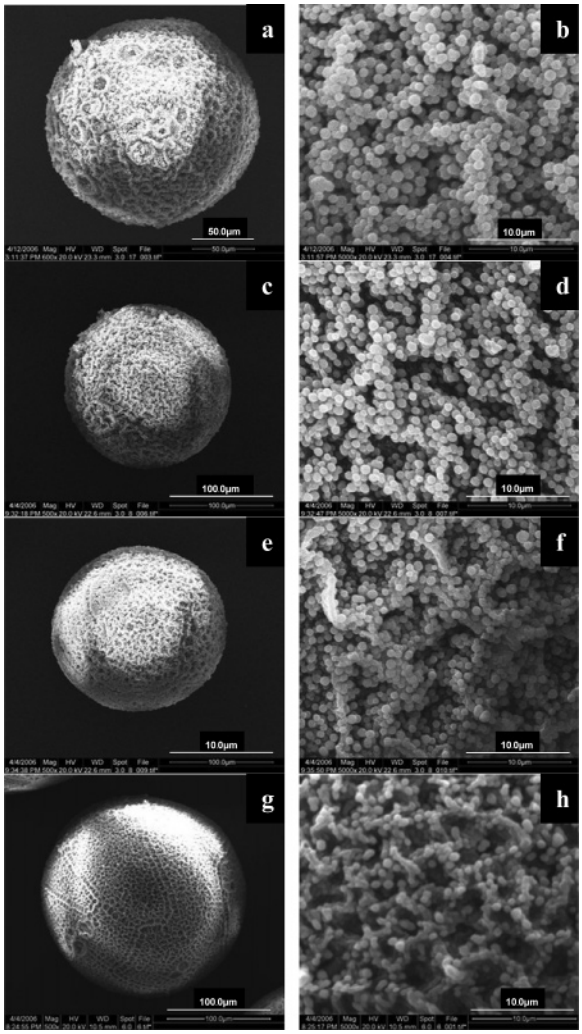


**Figure 3.** SEM images of the composite microspheres prepared in different TBOT concentrations. TBOT concentration was controlled by the change in the volume ratio of TBOT to anhydrous alcohol: (a, b) 0.02, (c, d) 0.01, (e, f) 0.005, and (g, h) 0.003.

On the basis of the above explanations, the reason for the effect of BA concentration on the morphology of the composite microgels is essentially related to the amount of residual impregnation liquid in the template microgels. A similar phenomenon could be observed in the experiments concerning the influence of the amount of residual impregnation liquid on the morphology of composite microspheres.

**Influence of the Amount of Residual Impregnation Solution on the Morphology of the PAM/$TiO_2$ Composite Microspheres.** Employing the proposed method for the preparation of PAM/$TiO_2$ composite microspheres, the morphology of the composite microspheres is affected not only by the TBOT concentration in the residual impregnation

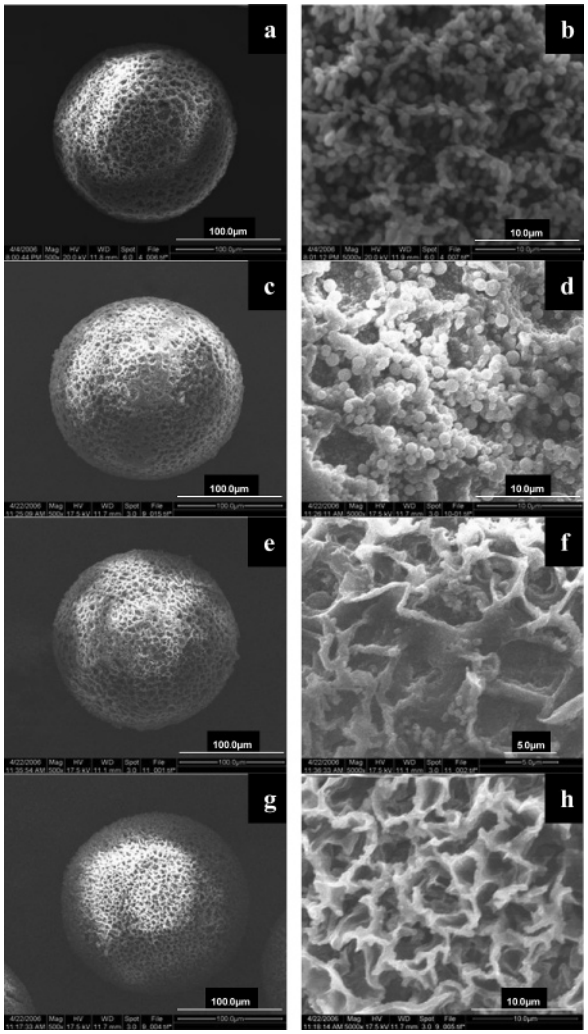


**Figure 4.** SEM images of the composite microspheres prepared in different amounts of residual impregnation liquid. The amount of residual impregnation liquid controlled by vacuuming time was (a, b) 10, (c, d) 20, (e, f) 30, and (g, h) 40 min.

solution but also by the amount of the residual impregnation solution in the template microspheres. Although the hydrolysis and condensation of TBOT occurs at the surface of the template microspheres, the pores of the template microspheres can be used as solution pools, if the pores of microspheres are filled with impregnation solution. In this situation, the hydrolysis and condensation could eventually take place in the liquid phase. So, a microenvironment for the formation of $TiO_2$ directly depends on the amount of impregnation solution in the microgels. It is obviously not hard to imagine that it is very difficult to form $TiO_2$ particles in larger sizes if the pores lack solvent. To get the uniformly immersed microspheres and the effectively controllable impregnation solution into the pores of the microspheres, the process mentioned in section 2.4 was carried out. The template microspheres, which were fully immersed into TBOT anhydrous alcohol solution, were vacuumed for a given time, and the resulting product was placed in a moist atmosphere with a given humidity (see Table 1). Finally, the desired composite microspheres were obtained.

Figure 4 indicates the SEM images of PAM/$TiO_2$ composite microspheres prepared in case of different vacuuming times when the other experimental conditions were fixed. All conditions are shown in Table 1. From Figure 4, the following results were found. The surface pattern of the composite microspheres is uniform, indicating that the method for the preparation of the composite microspheres is matched with the well-distributed impregnation liquid in the template microspheres. Obviously, the size of each $TiO_2$ particle decreases with increased vacuuming time. Comparing Figure 3a with Figure 4g, this phenomenon is more striking. It was hard to find the $TiO_2$ particles when the vacuuming time was 40 min (see Figure 4g). However, in the case of the immersed template microspheres, without vacuum treatment, the $TiO_2$ particles in larger sizes densely covered the surface of the composite microspheres (see Figure 3a). Interestingly, it seems that the surface morphologies of composite microspheres are topologically related to the porous morphologies of PAM microspheres. With the increase in vacuuming time, the morphology of the composite microspheres gradually changes to the morphology of the template microspheres. For example, in the case of the vacuuming time being 40 min, the porous structure of the composite microspheres (see Figure 4h) is very similar to that of the PAM microspheres (see Figure 2f). However, the pore wall of the composite microspheres is thicker than that of PAM template microspheres. This difference is related to the deposition of $TiO_2$ in the composite microspheres. Although the particles of $TiO_2$ in the composite microspherse, in the case of the 40 min vacuum time, are hardly found, the EDX analysis shown in Figure 8 obviously verifies the presence of $TiO_2$ in the composite microspheres.

On the basis of this set of experiments, the following conclusions are obtained. (1) The pore size and surface morphologies of the composite microspheres could be controlled by changing the amount of residual impregnation liquid in the template. (2) The larger the amount of residual solution that is located in the template, the more easily condensation occurs between the hydrolytes, therefore forming $TiO_2$ particles in larger sizes on the template microspheres. (3) Once the other conditions have been fixed, when one wants to achieve formation of the composite microspheres with porous structures, changing the amount of residual impregnation liquid in the template is more efficient than altering the precursor concentration in the impregnation liquid.

**Influence of Humidity on the Morphology of the PAM/$TiO_2$ Composite Microspheres.** According to the proposed method for preparation of PAM/$TiO_2$ composite microspheres, the interfacial reaction between TBOT located at the immersed PAM microspheres and water in a moist atmosphere is employed to incorporate $TiO_2$ into the template microspheres. So, it is necessary to investigate the effect of humidity on the morphology of the composite microspheres. To control the humidity in the gas phase, we placed the mixture of anhydrous alcohol and water in different volume ratios in a closed beaker to create different humidity levels in the gas phase. Some conditions for the preparation of composite microspheres under different humidity conditions are shown in Table 1, in which the volume ratios of water to alcohol for controlling the humidity are 1:0, 7:3, 1:1, and 3:7. The SEM images of PAM/$TiO_2$ composite microspheres

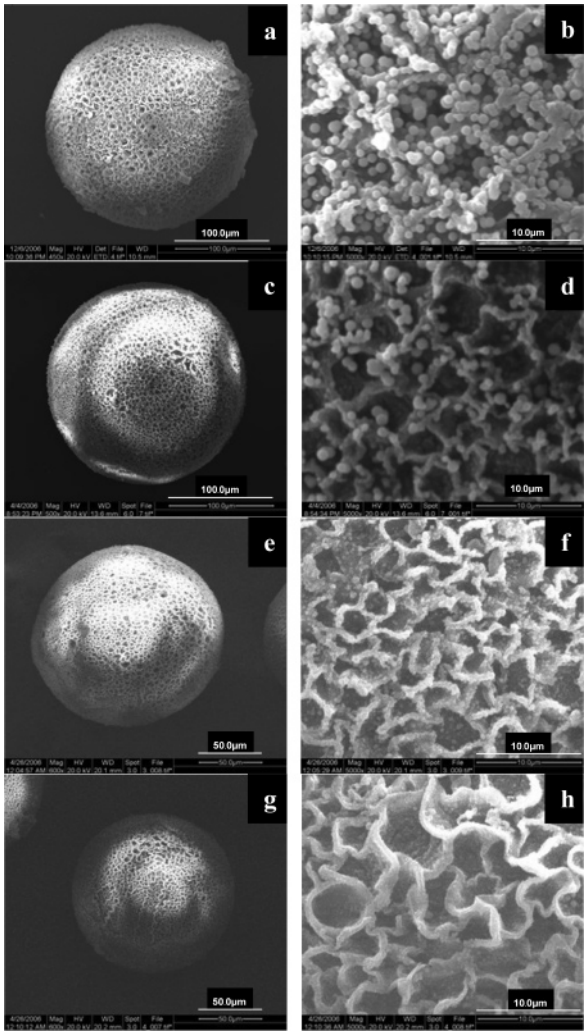


**Figure 5.** SEM images of the composite microspheres prepared in different humidity. The humidity controlled by the change in the volume ratio of water to alcohol: (a, b) 1:0 (c, d) 7:3 (e, f) 1:1, and (g, h) 3:7.

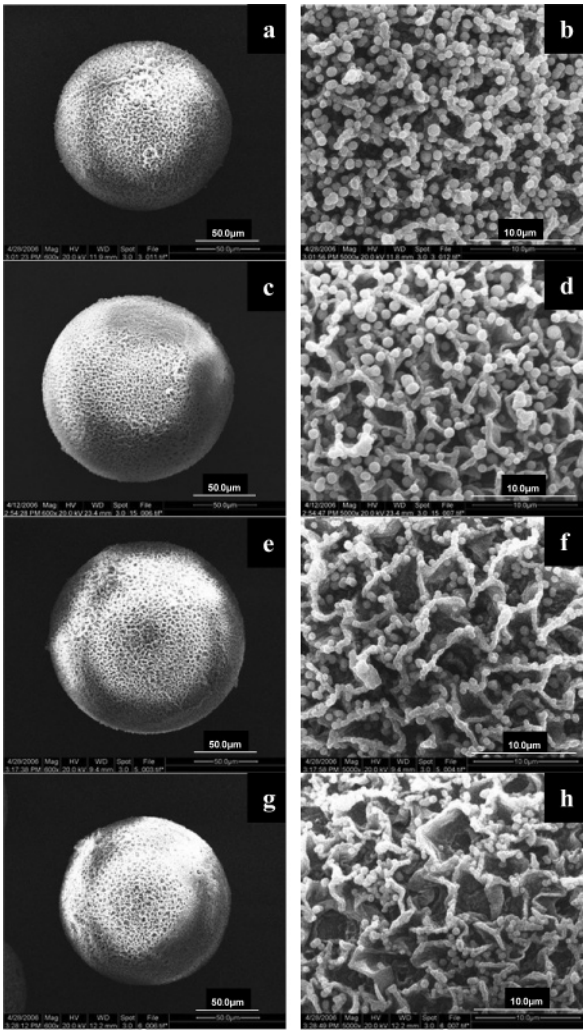


**Figure 6.** SEM images of the composite microspheres prepared using the freeze-dried PAM microspheres with different cross-linking degrees as templates. The cross-linking degree was controlled by the changing amount of BA (cross-linker): (a, b) 0.084, (c, d) 0.072, (e, f) 0.048, and (g, h) 0.036 g.

prepared at different humidity levels are shown in Figure 5. As expected, the regular variety in the surface morphologies of the composite microspheres was found. With a decrease of the volume ratio, a significant decrease in both the number and size of $TiO_2$ particles deposited on the surface of composite microspheres were observed, and the porous structures of the composite microspheres gradually became obvious.

These observations could be explained in terms of the difference in rate between the hydrolysis and volatilizing solvent. With a decrease in the volume ratio of water to alcohol in the mixture, the water content in the gas phase decreases. In this case, less water does not facilitate the hydrolysis of TBOT. Moreover, there is an increase in the amount of the volatilizing solvent from the immersed template microgels. Consequently, both factors result in, not only the preferable deposition of $TiO_2$ on the pore wall of the template microspheres, but also the favorable formation of $TiO_2$ particles in smaller sizes. The results from these experiments indicate that the surface morphologies of the composite microspheres can be effectively adjusted by controlling the humidity in the gas phase. In our opinion, the variation in the amount of residual impregnation solution, caused by volatilizing solvent in different humidity, is probably one of the primary factors for morphological change. Therefore, the SEM images of the composite microspheres, prepared in different amounts of residual impregnation liquid as shown in Figure 4, are similar to that of in different humidity as shown in Figure 5.

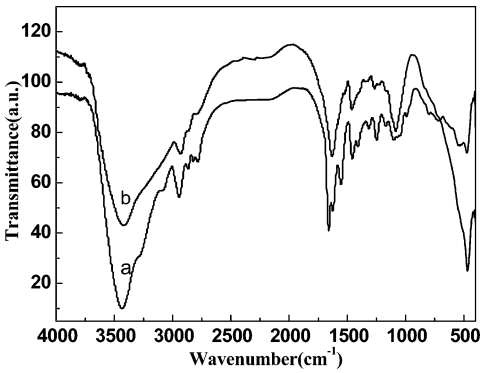


**Figure 7.** Typical FT-IR spectra of (a) PAM microgels and (b) PAM/$TiO_2$ composite microspheres.

**Influence of Cross-Linking Degree on the Morphology of the Composite Microspheres.** As mentioned in section 3.1, the pore size of freeze-dried PAM microspheres depends

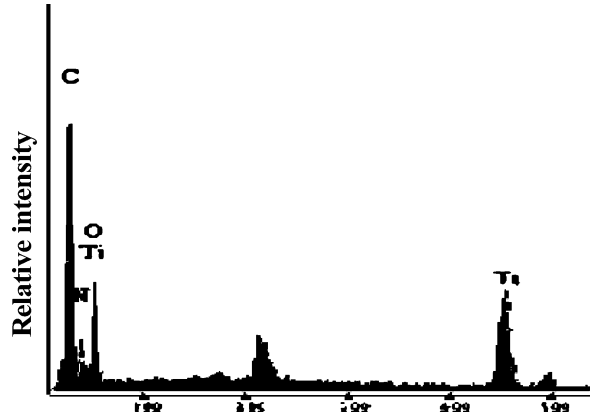


**Figure 8.** EDX spectrum of PAM/$TiO_2$ composite microspheres prepared in the conditions shown in Table 1 (Figure 4g).

upon the cross-linking degree of the PAM microspheres. So, employing the freeze-dried PAM microspheres with different cross-linking degrees as templates is one of the efficient methods of preparing the composite microspheres with different morphologies. PAM microspheres with different cross-linking degrees were made by changing the BA content in the preparation of PAM microgels. Figure 6 shows the SEM images of PAM/$TiO_2$ composite microspheres prepared by using the freeze-dried PAM microgels with different cross-linking degrees as templates. All conditions for the preparation of the composite microspheres are shown in Table 1.

It can be seen in Figure 6 that the pore size of composite microspheres increases with the decrease of BA. This phenomenon is similar to that observed in Figure 2. These results imply that the surface morphology of PAM/$TiO_2$ microspheres is directly related to that of the freeze-dried PAM microgels. As discussed in the section 3.1, the pore structure of the freeze-dried PAM microspheres is hardly affected by anhydrous alcohol. Therefore, the framework of the freeze-dried PAM microspheres would be maintained when the freeze-dried PAM microspheres were immersed in the mixture of TBOT and alcohol. Regarding the decrease in the number of $TiO_2$ particles with decrease in BA, observed in Figure 6, it could be attributed to the following reasons.

When the pore sizes of the template microspheres are larger, the confined $TiO_2$ particles formed in the impregnation solution are not enough to fill with pores of the template microspheres, but on the contrary, the pores are filled with $TiO_2$ particles. The difference in morphologies of the composite microspheres shown in Figures 6h, 4h, and 5h should be noted. It can be found in Figure 6h that there are obvious $TiO_2$ particles in the pores of the composite microspheres. However, $TiO_2$ particles are difficult to find in Figure 5h, and especially in Figure 4h. These differences are attributed to the variations in the amounts of impregnation solution. In the cases of Figures 5h and 6h, there was a certain amount of impregnation solution in the PAM microgles due to the composite microspheres prepared without vacuum processes. As a result, the formation of $TiO_2$ particles in larger sizes was favorable. In contrast, in the case of Figure 4h, the vacuum treatment was used for preparation of the composite microspheres, which resulted in a lack of the impregnation solution in the PAM microgles. Accordingly, the formation of $TiO_2$ particles was unfavorable. On the basis of these methods, the pore size of the PAM/$TiO_2$ composite microspheres and the sizes of $TiO_2$ particles can be controlled.

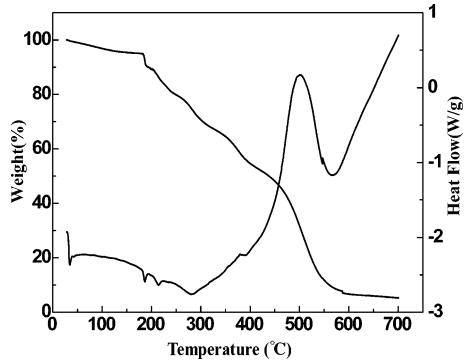


**Figure 9.** The typical thermogravimetric curve and DSC curve for the PAM/$TiO_2$ composite microspheres.

**3.3. Analysis of Components and Characterization of Porous Scaffolds.** The techniques including FT-IR, EDX, TGA, XRD, BET, and mercury intrusion porosimetry would be used for characterizations of PAM microspheres and the PAM/$TiO_2$ composite microspheres. The results obtained from these characterizations are as follows with examples to show some general information on the composite microspheres.

**FT-IR Analysis.** Figure 7 shows typical FT-IR spectra of PAM microgels (a) and PAM/$TiO_2$ composite microspheres (b). The characteristic absorption bands for PAM are clearly observed in plots a and b of Figure 7. The characteristic peaks are at 1658 $cm^{-1}$ ($\nu_{C=O}$), 2944 $cm^{-1}$ ($\nu_{CH_2}$), 1458 and 1409 $cm^{-1}$ ($\delta_{CH_2}$), and 3500−3300 $cm^{-1}$ ($\nu_{NH}$), which confirm that PAM exists in the composite materials. The spectra are consistent with that of the literature.[44] Compared with Figure 7a, a strong absorption band between 500 and 900 $cm^{-1}$, originating from the titanium dioxide,[45] is found in Figure 7b, indicating that $TiO_2$ incorporates with PAM microgels.

**EDX Analysis.** To get information about change in elements before and after the incorporation of $TiO_2$, PAM/$TiO_2$ composite microspheres prepared in the conditions shown in Figure 4g as examples were examined by EDX analysis. The result is shown in Figure 8. The obvious characteristic peaks for C, N, O, and Ti elements, originating from composite microspheres, are found in Figure 8, indicating that $TiO_2$ is, indeed, incorporated in the PAM microspheres.

**TGA Analysis.** Thermogravimetric analysis is useful for determining the content of inorganic components in composite materials. Herein, a typical thermogravimetric curve of the PAM/$TiO_2$ composite microspheres, as an example, is given in Figure 9. The result shows that a loss of 5.1% in weight, below 200 °C, is assigned to releasing water physiabsorbed in the composite microspheres.[46] From 200

(44) Zhu, J. F.; Zhu, Y. J. *J. Phys. Chem. B* **2006**, *110*, 8593.
(45) Zhang, Y. X.; Li, G. H.; Wu, Y. C.; Luo, Y. Y.; Zhang, L. D. *J. Phys. Chem. B* **2005**, *109*, 5478.
(46) Tang, W. P. *J. Mater. Chem.* **2004**, *14*, 4357.

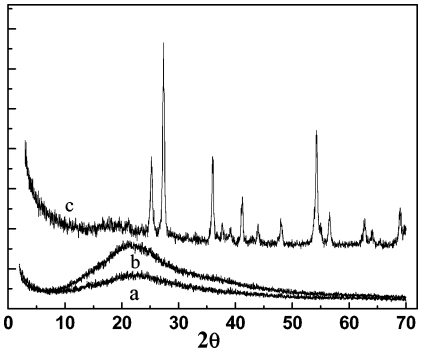


**Figure 10.** Typical XRD patterns of (a) PAM, (b) PAM/$TiO_2$, (c) and PAM/$TiO_2$ after calcination at 600 °C.

to 600 °C, a loss of 88.6 wt % could be ascribed to the decomposition of PAM and loss of water from crystal transformation. There is an obvious decrease in weight in the range from 200 to 550 °C, with an obvious endothermal peak at 500 °C, the weight loss being mainly related to the decomposition of PAM in composite microspheres.[47,48] Additionally, from 200 to 300 °C, there is a loss of water due to the decomposition of the amorphous hydrolytic compound in forming anatase-type $TiO_2$ crystals.[49] An obvious endothermal phenomenon above 550 °C, without obvious weight loss, is related to the transformation of anatase $TiO_2$ into rutile $TiO_2$.[50] The final residue is about 6.3 wt %, which is assigned to the total weight of $TiO_2$ in the composite materials.

**XRD Analysis.** To get some information on $TiO_2$ in the composite microspheres, we analyzed some samples by XRD. The typical X-ray diffraction (XRD) patterns for different samples, including PAM microgels (a), PAM/$TiO_2$ composite microspheres (b), and PAM/$TiO_2$ composite microspheres after calcination at 600 °C for 5 h (c), are shown in Figure 10.

No diffraction peaks in the spectra for the PAM microgels and PAM/$TiO_2$ composite microspheres were found (see plots a and b in Figure 10), suggesting that PAM and titanium dioxide are amorphous. In contrast, a number of sharp peaks were found, in the case of PAM/$TiO_2$ composite microspheres after calcination at 600 °C for 5 h (see Figure 10c), indicating that there are crystalline materials in the sample. The different peaks at $2\theta$ are 25.241, 27.359, 36.038, 41.279, and 54.319, respectively. The finding XRD data indicate that the residue is a mixture of the rutile form (JCPDS. 21-1276) and anatase form (JCPDS 21-1272). The result implies that the phase transformation from anatase to rutile was uncompleted in the given experimental conditions.

**BET Analysis and Mercury Intrusion Porosimetry.** The composite microspheres with macropores are found in SEM images. However, micropores might exist in the walls of these macropores. Considering that there are both macropores and micropores in the composite microspheres, the pore parameters related to the micropores and macropores were determined by BET and mercury intrusion porosimetry, respectively. Herein, the freeze-drying PAM microspheres, prepared in conditions shown in Table 1 (Figure 2g) and PAM/$TiO_2$ composite microspheres prepared in conditions shown in Table 1 (Figure 4g), as examples, were selected to determine the pore parameters. The results are shown in Tables 2 and 3 and Figures 11 and 12.

Table 2 shows the micropores parameters determined by BET. It can be seen in Table 2 that the pore diameters, with nanoscales present in both microspheres, confirm its fine porosity. To make a comparison of the pore sizes shown in Figures 2g and 4g, the pore diameters shown in the Table 2 are smaller. So, the pore diameters determined by BET are ascribed to the micropores in the walls of the macropores. For PAM microspheres, the specific surface area and porous volume are smaller than that of PAM/$TiO_2$ composite microspheres, which is attributed to the presence of amorphous $TiO_2$ in the composite microspheres. The similar pore diameters for PAM microspheres and PAM/$TiO_2$ composite microspheres imply that the micropore diameters of amorphous $TiO_2$ are similar to that of polymeric scaffolds.

The micropore size distribution curves of the PAM microspheres and the composite microspheres are shown in plots a and b of Figure 11, respectively. It obviously indicates that the micropore size distributions are not monomodals, with several maxima appearing in the distribution functions, and that the pore size scales are less than 100 Å. Additionally, the micropore size distribution of the PAM microspheres is more decentralized than that of the composite microspheres. A probable reason is that the pores in the composite microspheres, with a range from 40 to 100 Å, are filled with $TiO_2$ particles. It is the same reason that makes the micropore sizes in PAM microspheres, with a range from 14 to 39 Å, correspondingly shift to smaller sizes in the composite microspheres. It can be found in Figure 11 that the most probable micropore sizes of the PAM microspheres and the composite microspheres are 8.28 and 10.18 Å, respectively.

Table 3 shows the parameters of the macropores that are determined by mercury intrusion porosimetry. From Table 3, it can be found that total intrusion volumes and porosities, for PAM microspheres, are similar to those of the composite microspheres. However, it clearly indicates that the average pore diameters and total pore areas, for PAM microspheres, are different from those of the PAM/$TiO_2$ composite microspheres. These differences are attributed to filling $TiO_2$ into the polymer scaffolds of the composite microspheres. Especially, the total pore area of PAM/$TiO_2$ composite microspheres is significantly enhanced. The average pore diameters for both PAM microspheres and PAM/$TiO_2$ composite microspheres occur primarily in the micrometer scale, indicating that there are macropores in both microspheres. These results are generally concordant with those of the SEM images (reseef Figures 2h and 4h). The distributions of pore sizes determined by mercury intrusion porosimetry, shown in Figure 12, verify these results.

From Figure 12, it appears that the pore sizes, in the PAM microspheres and PAM/$TiO_2$ composite microspheres, fall into the macropore pore size (>50 nm). Moreover, the pore

(47) Minsk, L. M.; Kotlarchik, C.; Meyer, G. N.; Kenyon, W. O. *J. Polym. Sci., Part A: Polym. Chem.* **1974**, *12*, 133.
(48) Conley, R. T.; Mallo, R. In *Thermal Stability of Polymers*; Conley, R. T., Ed.; Marcel Dekker: NewYork. 1970; Vol. 1, p 254.
(49) Dussert, A.; Gooris, E.; Hemmerle, J. *Int. J. Cosmet. Sci.* **1997**, *19*, 119.
(50) Jiang, D. L. Ph.D. Thesis, School of Environmental and Applied Sciences, Griffith University, Australia, June 2004.

**Table 2. Micropore Parameters Determined by BET**

| sample | specific surface area ($m^2/g$) | porous volume ($cm^3/g$) | mean pore diameter (Å) |
|---|---|---|---|
| PAM microspheres* | 1.2 | 0.01 | 30.55 |
| PAM/$TiO_2$ composite microspheres[b] | 5.611 | 0.03 | 30.11 |

[a] The conditions for preparation of PAM microspheres are shown in Table 1 (Figure 2g). [b] The conditions for preparation of the PAM/$TiO_2$ composite microspheres are shown in Table 1 (Figure 4g).

**Table 3. Macrospores Parameters Determined by Mercury Intrusion Porosimetry**

| pore parameters | PAM microspheres[a] | PAM/$TiO_2$ composite microspheres[sb] |
|---|---|---|
| total intrusion volume (mL/g) | 2.9368 | 2.7943 |
| total pore area ($m^2/g$) | 17.608 | 83.310 |
| average pore diameter (4V/A) ($\mu$m) | 0.6671 | 0.1342 |
| porosity (%) | 74.0188 | 76.0650 |

[a] The conditions for preparation of the PAM microspheres are shown in Table 1 (Figure 2g). [b] The conditions for preparation of the PAM/$TiO_2$ composite microspheres are shown in Table 1(Figure 4g).

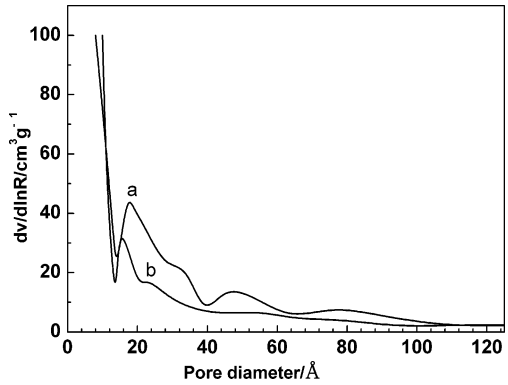


**Figure 11.** Micropore size distribution curves of (a) the porous PAM microspheres prepared in the conditions shown in Table 1 (Figure 2g) and (b) the composite microspheres prepared in the conditions shown in Table 1 (Figure 4g).

size distributions for the two microspheres are polymodal and all peaks correspond to macropores. For PAM microspheres, the peaks locate at 0.021, 0.095, 3.19, and 7.91 $\mu$m, respectively (see Figure 12a and its inset), and the pore sizes with a range from 5 to 20 $\mu$m are dominant (see Figure 12a). For PAM/$TiO_2$ composite microspheres, the peaks locate at 0.12, 2.79, and 7.91 $\mu$m (see Figure 12b and its inset), and the dominant pore sizes are similar to those of PAM microspheres (see Figure 12b). These results agree with those of the SEM images shown in Figures 2h and 4h. Additionally, it is found that the peak at 0.021 $\mu$m in the inset of Figure 12a disappears in the inset of Figure 12b. These results imply that the incorporation of the small-sized $TiO_2$ into PAM microspheres strongly affects the micropore size distribution of the polymer scaffolds. On the basis of these results, it is easier to understand that the incorporation of the larger-sized $TiO_2$ PAM microspheres should significantly influence the macropore size distribution of the freeze-drying PAM microspheres.

## 4. Conclusions

This was the first method proposed by us regarding the preparation of PAM/$TiO_2$ composite microspheres with controllable surface morphologies. PAM/$TiO_2$ composite microspheres with hierarchical surface structures were synthesized by the reaction between tetrabutyl titanate (TBOT) located within the porous polyacrylamide (PAM) microgels and water in a moist atmosphere.

The effects of the amount of the cross-linker BA, the concentration of TBOT solution, the humidity of the gas

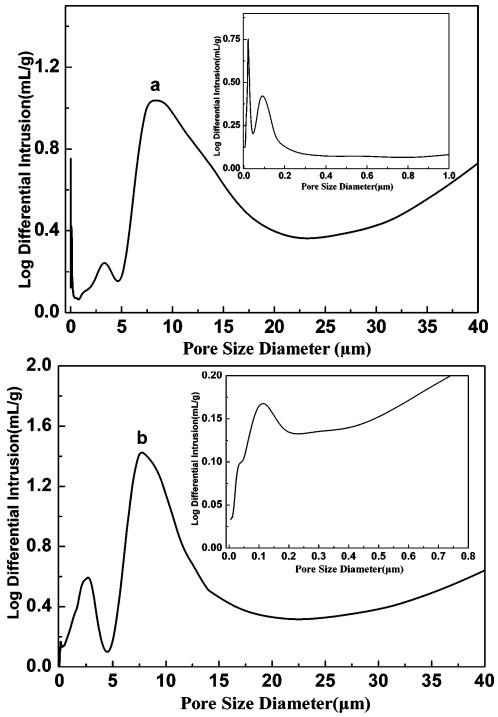


**Figure 12.** Macropore size distribution curves of (a) the porous PAM microspheres prepared in the conditions shown in Table 1 (Figure 2g) and (b) the composite microspheres prepared in the conditions shown in Table 1 (Figure 4g).

phase, as well as the amount of residual impregnation liquid on the morphologies of composite microspheres were investigated. The results indicate that the surface morphologies of composite microspheres can be effectively adjusted by changing the amount of BA. The pore size of the PAM microgels decreases with the increase of BA. On the basis of this kind of template microsphere, the pore size of PAM/$TiO_2$ composite microspheres can be relevantly adjusted. The morphologies of the composite microspheres gradually tend toward that of the template microspheres with a decrease in the impregnation liquid. Therefore, the pore size and surface morphologies of composite microspheres can be also adjusted by means of controlling the amount of residual impregnation liquid in the template microspheres. Regarding the effect of TBOT concentration on the morphology of the composite microspheres, the surface of the composite microspheres is densely covered by $TiO_2$ particles, when the TBOT concentration is high in the impregnation liquid. With the decrease in TBOT concentration, the number of $TiO_2$ particles

deposited on the composite microspheres decreases and most of the $TiO_2$ particles were deposited on the inner walls of the pores with the result that the surface morphology of the composite microspheres appear as an obviously porous structure. With an increased amount of water in a gaseous atmosphere, $TiO_2$ particles deposited on the surface of composite microspheres decrease both in number and size and the porous structures of the composite microspheres become obvious.

The composite microspheres, with three typical surface morphologies, were obtained by changing the parameters mentioned above:

(1) A wrinkly surface is covered by dense larger-sized $TiO_2$ particles.

(2) A porous surface is sparsely suffused by $TiO_2$ larger-sized particles, found both in the corrugations and the inner walls of porous channels.

(3) An obvious macroporous surface is distributed everywhere in smaller-sized $TiO_2$ particles.

The size of the $TiO_2$ particles and the morphology of the composite microspheres can be easily adjusted, and the incorporation of $TiO_2$ into PAM microspheres makes an obvious increase in the specific surface area of the composite microspheres. The pore size distribution of the composite microspheres strongly depends on the sizes of the $TiO_2$ particles. Moreover, this technique is suitable for the fabrication of various composite materials by altering precursors and polymeric microgel templates.

**Acknowledgment.** The authors thank the NSF of China (20576068), SRF for ROCS, SEM, and the NSF of Shaanxi Province (2005B12) for financial support.

CM062561G